Proceedings of the 9th U.S. National and 10th Canadian Conference on Earthquake Engineering
Compte Rendu de la 9ième Conférence Nationale Américaine et
10ième Conférence Canadienne de Génie Parasismique
July 25-29, 2010, Toronto, Ontario, Canada • Paper No 1451

RECENT DEVELOPMENT OF EQUIVALENT FORCE CONTROL METHOD FOR HYBRID TESTING

B. Wu[1], G. S. Xu[2], L. X. Deng[2], Z. X. Chen[3], Z. Wang[2], H. B. Jiang[4], H. D. Wang[1], F. L. Wang[1]

ABSTRACT

The equivalent force control (EFC) method replaces numerical iteration with a feedback control strategy to solve the nonlinear equations of motion in pseudo-dynamic and real-time substructure tests (RST) using an implicit integration method. The EFC method is briefly introduced first in this paper. Then the effectiveness and accuracy of the EFC method are reported with the full-scale quasi-static pseudo-dynamic tests of reinforced concrete (RC) shear wall structures and a reinforced masonry structure, and the RSTs of an offshore platform with MR damper specimen. It is shown that the EFC method can deliver excellent performance in all cases.

Introduction

In recent years, different approaches have been developed for real-time structural testing using servo-hydraulic actuators and reaction-wall or reaction-frame facilities. These include the effective force test method (Zhao et al. 2006) and real-time substructure test (RST) methods (Nakashima et al. 1992; Wu et al. 2005, 2006; Jung and Shing 2006). The latter is a hybrid experimental technique that combines numerical simulation with physical testing. While the effective force method is conceptually simple and does not require real-time numerical computation during a test, it is not as versatile as RST methods.

While many different numerical algorithms are available for RST (Darby et al. 2001; Wu et al. 2005, 2006), for structures with multiple degree of freedom (MDOF), an integration method with unconditional stability is highly desirable. Many implicit integration schemes are unconditionally stable but they require an iterative solution strategy for nonlinear systems, which is a challenge for RST. Implicit schemes have been implemented with different solution strategies to handle structural nonlinearity for RST, see, e.g., Shing et al. (2004), Bayer et al. (2005), Mosqueda and Ahmadizadeh (2007). Bayer et al. (2005) and Jung and Shing (2006) have used an unconditionally stable implicit time integration method with a specially designed nonlinear solution strategy that combines a Newton-type iterative method with subincrementation. To avoid spurious

[1]Professor, School of Civil Engineering, Harbin Institute of Technology, Harbin 150090
[2]PhD students, School of Civil Engineering, Harbin Institute of Technology, Harbin 150090
[3]Lecture, School of Civil Engineering, Harbin Institute of Technology at Weihai, Weihai 264209
[4]Associate Professor, School of Civil Engineering, Harbin Institute of Technology, Harbin 150090

loading and unloading of a specimen, the commands for the actuators are generated by a quadratic (Jung and Shing 2006) or linear (Bayer et al. 2005) interpolation based on iterative trial quantities.

To avoid the numerical iteration process associated with implicit integration, Wu et al. (2007) have proposed the equivalent force control (EFC) method for RST. This paper describes basic concept of the EFC method, and recent applications to quasi-static pseudo-dynamic tests (PDT) and RST with various experimental substructures. These include a reinforced concrete (RC) shear wall, a three-story prefabricated RC shear wall structure, a three-story frame-supported reinforced masonry structure, and a MR damper specimen.

Overview of EFC Method

EFC with constant-average-acceleration method

The concept of the EFC method can be explained by expressing the numerical solution of the equations of motion with the constant-average-acceleration (CAA) method in the following form (Wu et al. 2007)

$$\mathbf{R}_{\mathrm{N}}(\mathbf{d}_{i+1}) + \mathbf{K}_{\mathrm{PD}}\mathbf{d}_{i+1} + \mathbf{R}_{\mathrm{E}}(\mathbf{a}_{i+1}, \mathbf{v}_{i+1}, \mathbf{d}_{i+1}) = \mathbf{F}_{\mathrm{EQ},i+1} \tag{1}$$

where

$$\mathbf{K}_{\mathrm{PD}} = \frac{4\mathbf{M}_{\mathrm{N}}}{\Delta t^2} + \frac{2\mathbf{C}_{\mathrm{N}}}{\Delta t} \tag{2}$$

$$\mathbf{F}_{\mathrm{EQ},i+1} = \mathbf{F}_{i+1} + \mathbf{M}_{\mathrm{N}}\mathbf{a}_i + (\frac{4\mathbf{M}_{\mathrm{N}}}{\Delta t} + \mathbf{C}_{\mathrm{N}})\mathbf{v}_i + (\frac{4\mathbf{M}_{\mathrm{N}}}{\Delta t^2} + \frac{2\mathbf{C}_{\mathrm{N}}}{\Delta t})\mathbf{d}_i \tag{3}$$

In above equations, **d**, **v**, and **a** are the displacement, velocity, and acceleration vectors; $\mathbf{M}_{\mathrm{N}}$, $\mathbf{C}_{\mathrm{N}}$, $\mathbf{R}_{\mathrm{N}}$ are the mass matrix, damping matrix, and static restoring force vectors of the numerical substructure; $\mathbf{R}_{\mathrm{E}}$ is the restoring force vector of the experimental substructure including static, damping, and inertia forces; **F** is the external excitation force vector; and Δt the integration time interval; $\mathbf{K}_{\mathrm{PD}}$ is called the pseudo-dynamic stiffness, and $\mathbf{F}_{\mathrm{EQ}}$ the equivalent force (EF). The solution of Eq.1 can be interpreted as finding the response of a hybrid system, which consists of numerical and experimental substructures with real and pseudo-dynamic forces, to an explicit equivalent load. This response can be obtained by directly applying the equivalent force to the hybrid system, in which the numerical substructure and pseudo-dynamic forces are evaluated in a computer, using a force-feedback control strategy.

The block diagram representing an EFC system for a linear single-degree-of-freedom (SDOF) structure is shown in Fig. 1, in which K_{N} and K_{E} are the stiffness of the numerical and experimental substructures, respectively; C_{E} is the damping coefficient of the experimental substructure; and $T_{\mathrm{A}}(s)$ is the transfer function of the dynamics of the actuator-specimen system. The equivalent force controller shown in Fig. 1 is a proportional-integral-derivative (PID) controller, in which K_{P}, K_{I}, and K_{D} are the proportional, integral and derivative gains, respectively. The factor K_{F} after the equivalent force command $F_{\mathrm{EQ},i+1}$ is used to eliminate the steady-state error. After being processed by a EF controller, the force error e_{EQ} between the equivalent force command modified by K_{F} and the equivalent force feedback $F'_{\mathrm{EQ},i+1}$ is converted to a displacement command d^{c}_{i+1} by a conversion factor C_{F}. Then, the actuator is controlled with a displacement control mode. The term d'_{i+1} represents the displacement response of the

experimental substructure subjected to the command d^{c}_{i+1}. At the end of the (i+1)th step, the measured reaction force R_E and the calculated R_N is fed back to Eq.1 to calculate the displacement at this time step, and the corresponding velocity and acceleration responses of the structure are calculated according to the CAA method.

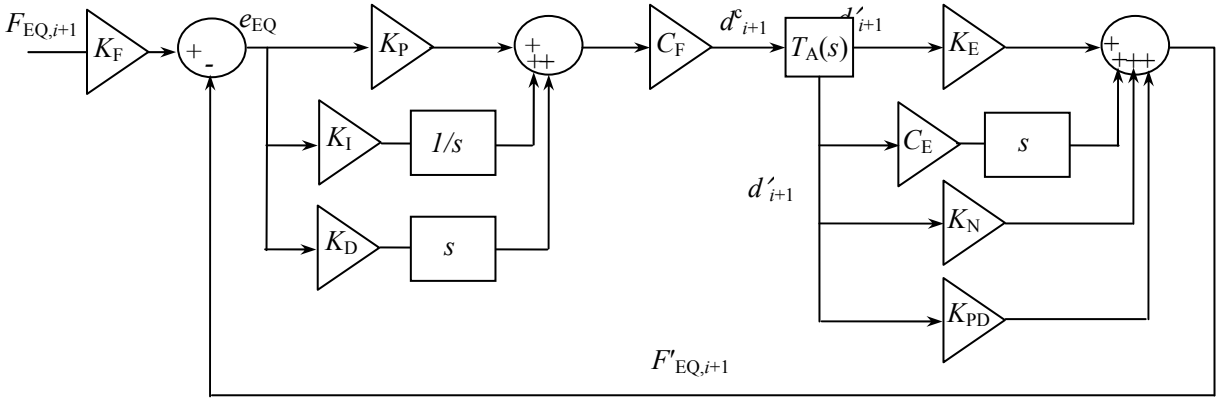

Figure 1. Block diagram of EFC with PID controller for a SDOF structure.

Based on Laplace's Terminal-Value Theorem (Ogata 2005), one can obtain the steady-state error of the whole system subjected to an EF input $F_{EQ,i+1}$. For the case of K_I=0, which means a P or PD controller is used, the steady-state error of the system subjected to a unit step EF command is $1/(1+K_P)$. Therefore, K_F should be equal to $(1+K_P)/K_P$ to eliminate the control error (Wu et al. 2007). For the case of $K_I \neq 0$, which means a PI or PID controller is used, the corresponding steady-state error is zero, requiring that K_F be equal to 1.

EFC with Implicit mid-point method

The EFC is not limited to be used with the CAA algorithm. The implicit mid-point method (IMM) is another unconditionally stable integration algorithm. When the IMM was employed in PDT with EFC, the equation of motion can be rearranged as

$$\mathbf{K}_{PD} \times \mathbf{x}_{i+1} + \mathbf{R}_N\left(\mathbf{x}_{i+1}\right) + \mathbf{R}_E\left(\mathbf{x}_{i+1}\right) = \mathbf{F}_{EQ,i+1} \tag{4}$$

in which

$$\mathbf{K}_{PD} = \left(\frac{4\mathbf{M}_N}{\Delta t^2} + \frac{2\mathbf{C}_N}{\Delta t}\right) \tag{5}$$

$$\mathbf{F}_{EQ,i+1} = \mathbf{F}_{i+\frac{1}{2}} + \left(\frac{4\mathbf{M}_N}{\Delta t^2} + \frac{2\mathbf{C}_N}{\Delta t}\right) \times d_i + \frac{2\mathbf{M}_N}{\Delta t} v_i \tag{6}$$

The block diagram of IMM-EFC is the same as Fig.1, but d should be replaced by x. The displacement and velocity at step (i+1) are determined with

$$\mathbf{d}_{i+1} = 2\mathbf{x}_{i+1} - \mathbf{d}_i \tag{7}$$

$$\mathbf{v}_{i+1} = \frac{2\mathbf{d}_{i+1} - 2\mathbf{d}_i}{\Delta t} - \mathbf{v}_i \tag{8}$$

Experimental Validations

To verify the accuracy and effectiveness of the EFC method, both PDTs and RSTs were conducted. The tests were performed at the Structural and Seismic Testing Center of Harbin Institute of Technology, in which a Flex Text GT controller was used to control a 2500kN MTS actuator or some 250-630kN Schenck actuators to impose displacement onto the specimen. The sampling frequency of the system was set to 2048Hz.

MR Damper Specimen

To suppress the vibration mainly induced by ice and earthquake loads, an isolation layer was designed between the main deck and top of the supporting jacket of the JZ20-2NW offshore platform located in Bohai Gulf of China. The photo of the platform is shown in Fig. 2. The detail of the isolation layer is shown in Fig. 3. It was composed of 8 rubber isolators and 8 MR dampers. The isolators were placed at the four corners and the center area of the isolation layer. The dampers were incorporated around the corners of the isolation layer. The platform model was simplified into an eight-degrees-of-freedom (8DOF) model as shown in Fig. 4. The structural parameters except for MR dampers can be found in Wu et al. (2008).

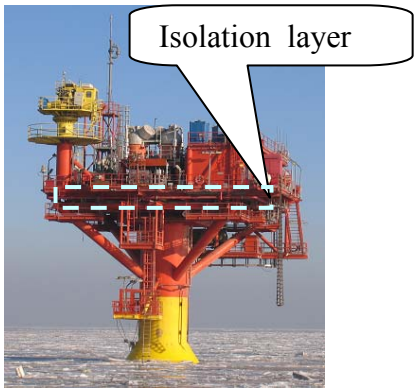

Figure 2. Photo of JZ20-2NW offshore platform.

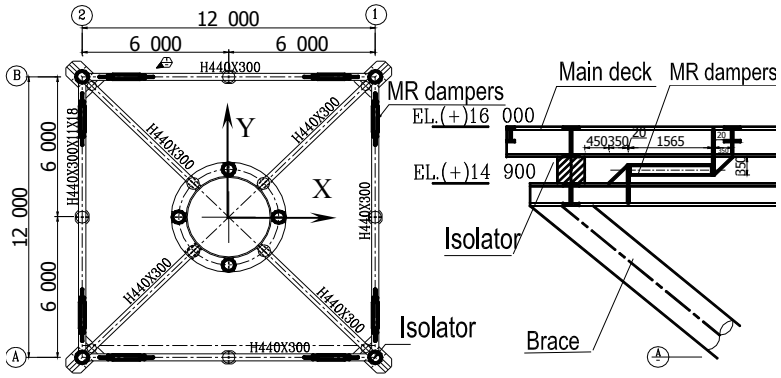

Figure 3. Isolation layer of JZ20-2NW platform.

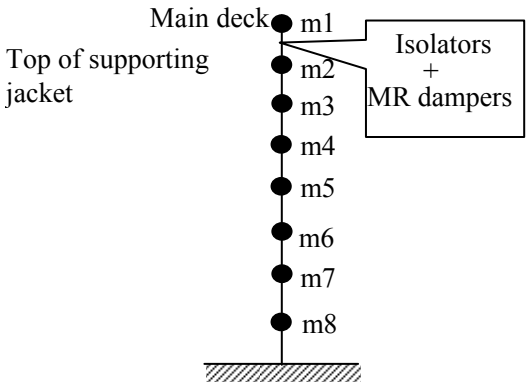

Figure 4. 8DOF model of the JZ20-2NW offshore platform.

Figure 5. Photograph of experimental setup with MR specimen.

For comparison, both the CAA-EFC and the CDM with conventional displacement control were used for the RSTs. The MR damper with zero drive voltage acting as a passive fluid viscous damper was the experimental substructure and the remainder of the structure was the numerical substructure. The test setup is shown in Fig. 5. The equivalent force command calculated with Eq.3 in each integration time step was divided into 20 sub-steps using linear interpolation in order to smooth the velocity response. The earthquake inputs were the El Centro (NS, 1940) and Taft (N21E, 1952) with peak acceleration of 1.00m/s^2, and Tianjin (1976) with peak acceleration of 0.35m/s^2. The control gain of the equivalent force controller was K_P=0.5. The integration time interval in the tests was chosen to be 0.02s.

The experimental drifts of the isolation layer subjected to El Centro (NS, 1940) earthquake are shown in Fig. 6. It is seen that the RST response with the CDM diverges, while that with the EFC method remains stable. The pure numerical result without dampers is also shown in Fig. 6, where the significant control effect of the dampers is observed. Fig. 7 shows hysteretic loops of the MR damper. Similar conclusions can be obtained from the tests of Taft (N21E, 1952) and Tianjin (1976) earthquake records.

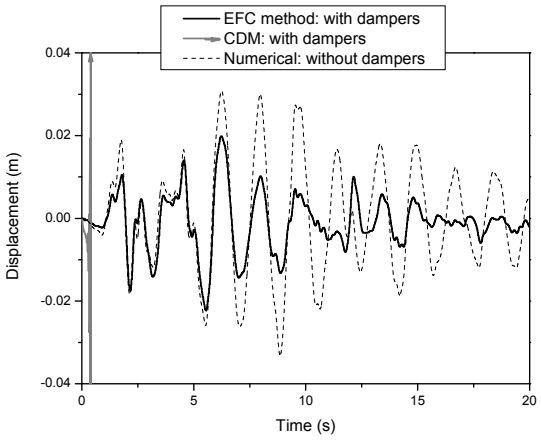

Figure 6. Drifts of the isolation layer.

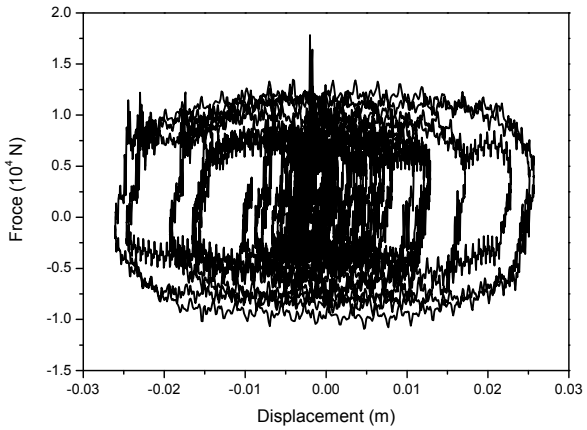

Figure 7. Hysteretic loops of MR damper.

RC Shear Wall Specimen

The PDT of the SDOF structure with a RC shear wall specimen was conducted with CAA-EFC. The structural parameters are M_N=9.43×10^{5}kg, K_N=1.019×10^{7}N/m, and C_N=5.922×10^{5}Ns/m. The precast RC shear wall was designed with a novel method for in situ connection of precast walls (Zhang 2009). The corresponding test setup is shown in Fig. 8. The parameters of the specimen are listed in Table 1. More information about this specimen can be found in Zhang (2009). The initial stiffness of the specimen obtained with preliminary quasi-static test is 2.7×10^{7}N/m. The circular frequency and damping ratio of the structure are 6.28rad/s and 5%, respectively. The integration time interval is 0.01s.

Table 1. Parameters of the precast RC shear wall specimen

Strength grade of steel bar	Strength grade of Concrete	Size of Specimen (mm×mm×mm)	Longitudinal Bar	Stirrup
HRB335	C30	2200×1400×200	12@200	8@200

The displacement responses of the structure subjected to El Centro (NS, 1940) ground motion with a peak acceleration of 0.5 m/s^2 are shown in Fig. 9. The EF controller gains are K_P=0.5 and K_I=10/s. Fig. 9 shows that the response of the actuator tracks its command well and the displacement response of the specimen matches closely with that of the structure. The obvious difference is also observed between displacement responses of the actuator and the specimen. The difference may be attributed to the slippage between the specimen and the strong floor to which it is attached. It is indicated from the good match of the responses of the specimen and the structure that the result from the EFC is reliable and the EFC method can effectively compensate for the specimen slippage if it is not fastened firmly enough to the floor. Fig. 10 shows the hysteretic loops of the specimen. The thin hysteretic loops imply its poor energy dissipation capacity after severe damages in the quasi-static cyclic test with large deformation prior to this PDT. The agreement of EF command and response depicted in Fig. 11 also shows the accuracy of the test result.

Figure 8. Test setup for RC shear wall specimen.

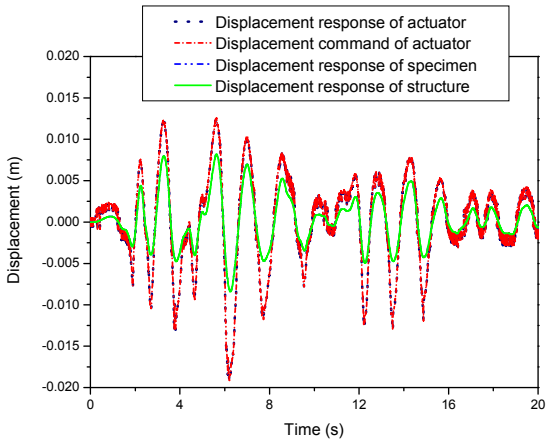

Figure 9. Comparisons of displacement histories.

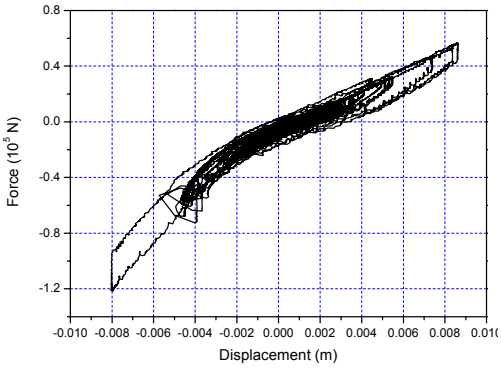

Figure 10. Hysteretic loops of the specimen.

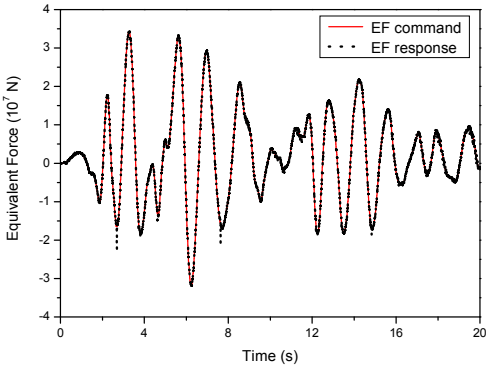

Figure 11. EF Command and response.

Three-story Precast RC Shear Wall Structure

A PDT of a three-story prefabricated RC shear wall structure was conducted with IMM-EFC and CDM. The floor masses are M_1=28.55×10^{3}kg, M_2=28.43×10^{3}kg, M_3=20.4×10^{3}kg, the initial stiffness of the stories obtained with preliminary quasi-static test are K_1=2.566×10^{7}N/m, K_2=1.092×10^{7}N/m, K_3=7.32×10^{6}N/m, and the damping matrix was determined by Rayleigh damping with the damping ratio equal to 0.05 for the fist and the second mode. Three 630kN

actuators and a 250kN actuator were used to impose displacements onto the specimen. The corresponding test setup is shown in Fig. 12.The EF controller gains are K_P=0.1 and K_I=25/s. The earthquake inputs were the WenChuan earthquake record with peak acceleration of 0.22m/s^2 when the loading rate is 100 times slower than the real time, and 0.11m/s^2 when 12 times slower. The integration time interval is 0.004s. The structure had experienced significant damage in the tests before this study.

The displacement commands, responses and reaction forces of the third floor are shown in Figs.13 to 18. It is can be see from Figs. 13 and 14 that when the time-scale equals 100 the response of the actuator tracks its command well for both the IMM and CDM. Nevertheless, an interesting result, when the loading rate increased, is seen from Figs. 17 and 18 that the reaction force with the CDM blows up to over 200kN in the first few seconds, while its counterpart with the IMM is restricted within 100kN.

Figure 12. Test setup for three-story prefabricated RC shear wall structure.

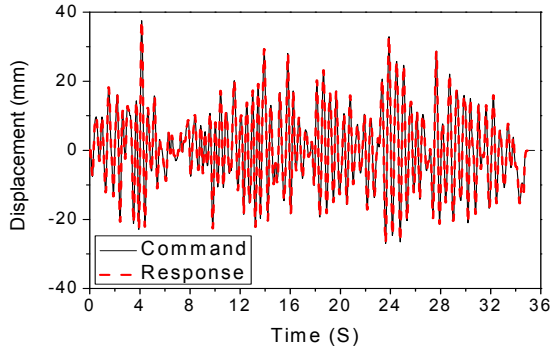

Figure 13. IMM with Time Scale=100:1.

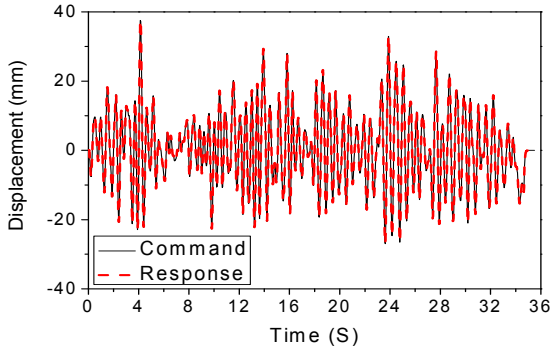

Figure 14. CDM with Time Scale=100:1.

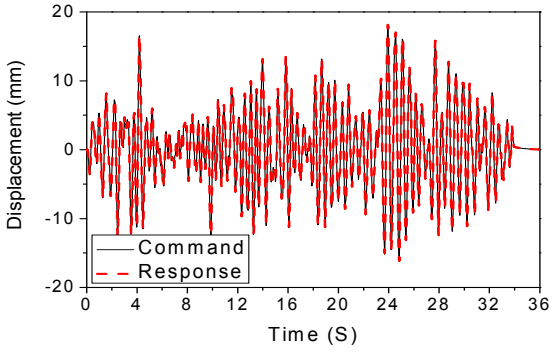

Figure 15. IMM with Time Scale=12:1.

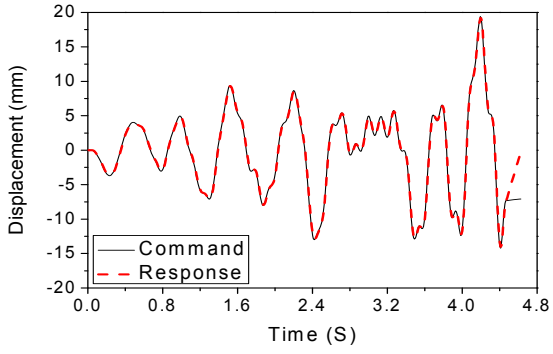

Figure 16. CDM with Time Scale=12:1.

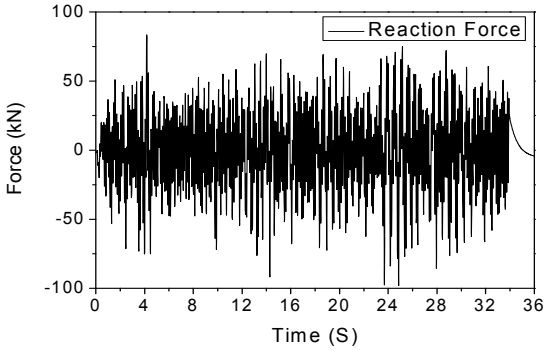

Figure 17. IMM with Time Scale=12:1.

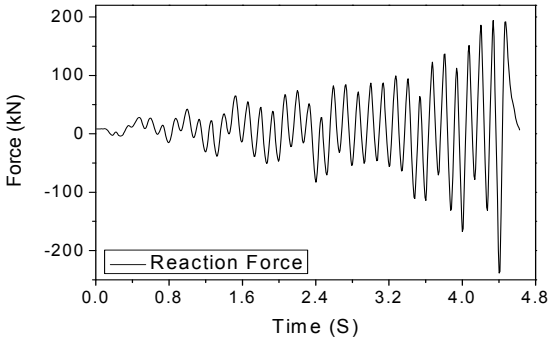

Figure 18. CDM with Time Scale=12:1.

Full-scale frame-supported reinforced masonry short-limb shear wall structure

This section presents the application of the proposed EFC method by a full-scale six-storey frame-supported reinforced masonry structure. The bottom three stories of the structure were chosen to be the physical substructure as shown in Fig. 19(a). The top three stories of the structure were modeled as the linear numerical substructure. Horizontal loading devices were three servo-hydraulic actuators with capacities of ± 630kN (± 250mm), ± 630kN (± 250mm) and ± 250kN (± 250mm) from top to bottom as shown in Fig. 19(b). Vertical loading was done by eight hydraulic jackets as shown in Fig. 19(c). El Centro (NS, 1940) with a peak acceleration of 220cm/s^2 was applied to the full-scale model for the PDT. The time interval of integration was set to 0.02s. The model parameters are shown in Table 2. The Rayleigh damping is obtained by:

$$\mathbf{C} = \alpha_0 \times \mathbf{M} + \alpha_1 \times \mathbf{K} \tag{9}$$

where $a_0 = 1.1615$ and $a_1 = 0.00142$.

Table 2 Testing Parameters of Structure

Floor No.	1	2	3	4	5	6
Mass(kg)	42100	35200	35200	35200	35200	20400
Initial stiffness(kN/mm)	63	155	235	422	422	422

(a) Testing model

(b) Horizontal loading device

(c) Vertical loading device

Figure19. Testing setup.

Fig.20 shows the overall view of equivalent force command and response on the first floor of the physical testing substructure. It is shown in this figure that the equivalent force response tracks the command well. However, the overshooting of equivalent force response can

be observed from close-up view of Fig. 20, as shown in Figs. 21 and 22. Even with the existence of overshooting at some time step, the EFC method can still achieved accurate result due to the contribution of PI controller. Fig. 23 shows the corresponding hysteretic loops of the specimen. Similarly results were obtained for the other two floors. It is clearly shown that the EFC method is effective for MDOF structure tests.

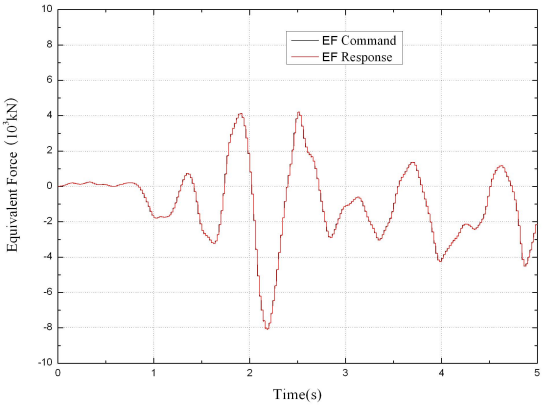

Figure 20. Overall view of equivalent force command and response.

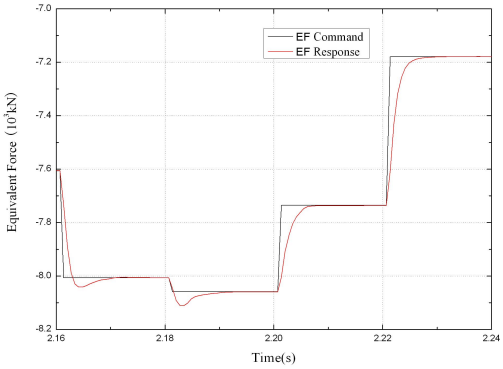

Figure 21. Equivalent force command and response between 2.16s and 2.24s.

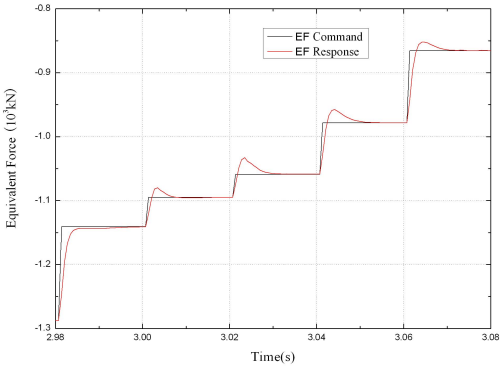

Figure 22. Equivalent force command and response between 2.98s and 3.08s.

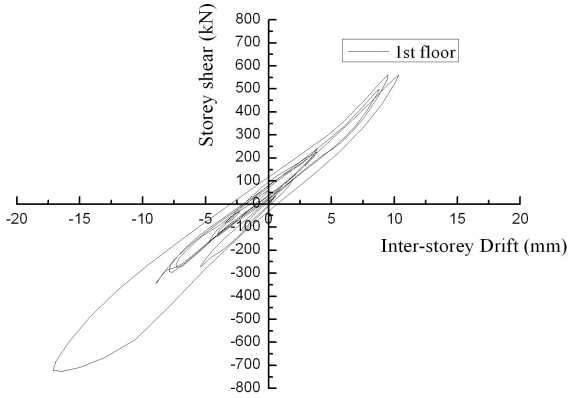

Figure 23. Hysteretic loops of physical substructure.

Conclusions

The basic idea of EFC for hybrid simulation is reviewed in this paper. The effectiveness and accuracy of the method were validated with the PDTs with a RC shear wall specimen, a three-story precast RC shear wall Structure and a frame-supported reinforced masonry structure, and with a RST of an offshore platform with MR damper specimen. It is shown that the EFC method can deliver robust and excellent performance for both RST and PDT of various structures.

Acknowledgments

This work was supported by Grant 90715036 and 50938001 from the National Science Foundation of China, and Grant 2008419073 from China Earthquake Ministration. The

assistance of Mr. Yunfei Ma and Mr. Darui Zhou of the Structural and Seismic Testing Center, Harbin Institute of Technology, with the operation of the MTS testing system is gratefully acknowledged.

References

Bayer, V., U. E. Dorka, U. Füllekrug, and J. Gschwilm, 2005. On real-time pseudo-dynamic sub-structure testing: algorithm, numerical and experimental results. *Aerospace Science and Technology* 9, 223–232.

Darby, A. P., A. Blakeborough, and M. S. Williams, 2001. Improved control algorithm for real-time substructure testing. *Earthquake Engineering and Structural Dynamics* 30, 431–448.

Jung, R. Y., and P. B. Shing, 2006. Performance evaluation of a real-time pseudodynamic test system. *Earthquake Engineering and Structural Dynamics* 35, 789–810.

Mosqueda, G., and M. Ahmadizadeh, 2007. Combined implicit or explicit integration steps for hybrid simulation. *Earthquake Engineering and Structural Dynamics* 36, 2325–2343.

Nakashima, M., H. Kato, and E. Takaoka, 1992. Development of real-time pseudo dynamic testing. *Earthquake Engineering and Structural Dynamics* 21, 79–92.

Ogata, K., 2005. Modern Control Engineering. *Prentice-Hall* (Reprinted by Tsinghua University Press, Beijing).

Shing, P. B., Z. Wei , R. Y. Jung, and E. Stauffer, 2004. Nees fast hybrid test system at the University of Colorado. *Proceedings of the 13th World Conference on Earthquake Engineering*. Vancouver, B.C., Canada, paper No. 3497.

Wu, B., H. Bao, J. Ou, and S. Tian, 2005. Stability and accuracy analysis of central difference method for real-time substructure testing. *Earthquake Engineering and Structural Dynamics* 34, 705–718.

Wu, B., G. S. Xu, Q. Y. Wang, and M. Williams, 2006. Operator-splitting method for real-time substructure testing. *Earthquake Engineering and Structural Dynamics* 35, 293–314.

Wu, B., Q. Y. Wang, P. B. Shing, and J. P. Ou, 2007. Equivalent force control method for generalized real-time substructure testing with implicit integration. *Earthquake Engineering and Structural Dynamics* 36, 1127–1149.

Wu, B., G. S. Xu, Y. Li, P. B. Shing, and J. P. Ou, 2008. Performance and application of equivalent force control method for real-time substructure testing. Submitted to *Journal of Engineering Mechanics (ASCE)*.

Zhang, H. S. 2009. Experimental study on lap-joint of steel bar of precast concrete shear walls. *Master's Thesis*, Harbin Institute of Technology. (in Chinese)

Zhao, J., C. French, C. Shield, and T. Posbergh, 2006. Comparison of tests of a nonlinear structure using a shake table and the EFT method. *Journal of Structural Engineering* 132(9), 1473–1481.